Regulatory network for cell shape changes during *Drosophila* ventral furrow formation

Julio Aracena[a,b], Mauricio González[c], Alejandro Zuñiga[c], Marco A. Mendez[c], Verónica Cambiazo[c,*]

[a]*Centro de Modelamiento Matemático, UMR-CNRS 2071, Universidad de Chile, Casilla 170-3, Santiago, Chile*
[b]*Departamento de Ingeniería Matemática, Universidad de Concepción, Casilla 160-C, Concepción, Chile*
[c]*Laboratorio de Bioinformática y Expresión Génica, INTA, Universidad de Chile, Macul 5540, Santiago, Chile*

Abstract

Rapid and sequential cell shape changes take place during the formation of the ventral furrow (VF) at the beginning of *Drosophila* gastrulation. At the cellular level, this morphogenetic event demands close coordination of the proteins involved in actin cytoskeletal reorganization. In order to construct a regulatory network that describes these cell shape changes, we have used published genetic and molecular data for 18 genes encoding transcriptional regulators and signaling pathway components. Based on the dynamic behavior of this network we explored the hypothesis that the combination of three recognizable phenotypes describing wild type or mutant cell types, during VF invagination, correspond to different activation states of a specific set of these gene products, which are point attractors of the regulatory network. From our results, we recognize missing components in the regulatory network and suggest alternative pathways in the regulation of cell shape changes during VF formation.

Keywords: *Drosophila* gastrulation; Ventral furrow; Boolean model; Cell shape changes

1. Introduction

The traditionally biological investigation has examined and collected information of a reduced number of genes, proteins or reactions. For years this approach has produced remarkable achievements and has allowed us to propose quite realistic biochemical models. However, with the advent of large sets of gene expression data generated by genomic and proteomic studies (Arbeitman et al., 2002; Gong et al., 2004) it has been evident that the identification of biologically meaningful gene or protein interactions involve novel approaches that go beyond the traditional experimental methods. One of these approaches is the building of genetic networks that model the actual behavior of the cells.

*Corresponding author. Tel.: +56 2 6781514; fax: +56 2 2214030.
E-mail address: vcambiaz@inta.cl (V. Cambiazo).

During recent years much has been learned about the genetic and molecular basis of gene networks controlling embryo development in *Drosophila* (Sauer et al., 1996). These networks involve hundreds of genes, which code for transcription factors, transmembrane receptors and their ligands, extracellular matrix proteins and components of intracellular signaling cascades (Casares and Sanchez-Herrero, 1995; Margolis et al., 1995; Bodnar, 1997; Sánchez and Thieffry, 2003; Thieffry and Sánchez, 2003).

In this work, we used published genetic and molecular data for 18 genes to construct a regulatory network for *Drosophila* ventral furrow (VF) formation, and we provide analyses of the dynamic behavior of this network by proposing a simple network that describes a regulatory pathway with on–off elements. We explore the hypothesis that the combination of the three recognizable phenotypes depicting the cell shape

changes that occur in wild type or mutant cells during VF invagination, namely: apico-basal nuclear movement, apical constriction and cell shortening, corresponds to the activation states of a specific set of gene products, which control the reorganization of the actin cytoskeleton in a single cell undergoing its own developmental program. In this work, the construction of the Boolean model as well as the inference of missed elements and structures has been based only on qualitative information, therefore it constitutes a first step towards our understanding of the emergent behaviors of interacting genes and gene products in the regulatory network that controls *Drosophila* VF formation.

1.1. Mathematical modeling of regulatory networks

Mathematical models that represent cellular processes or mechanisms have described some principles of the genetic networks. One of them summarizes the genetic regulatory network in terms of nodes—representing the genes—and connections among them that define the regulatory action of a gene product on another gene. Several of these models have been described as a two states or Boolean representation (Kauffman, 1969; Somogyi and Sniegoski, 1996; Wuensche, 1998).

In a Boolean idealized model, the activity of each element of the network is treated as a Boolean variable, where the value 1 corresponds to the activated state of the element and 0 to the inhibited state. The activation function of each element is a Boolean function, which depends on the values of the elements that participate in the regulatory network. In this work, we applied a particular type of activation functions called threshold functions, which are defined by

$$f_i(x) = H\left(\sum_{j=1}^{n} w_{ij}x_j - \theta_i\right), \tag{1}$$

where $x = (x_1, x_2, \ldots, x_n) \in \{0,1\}^n$, the coefficients w_{ij} and the number θ_i, called weights and threshold value, respectively, are real numbers, and H is the Heaviside step function:

$$H(x) = \left\{ \begin{array}{ll} 1 & \text{if } x > 0 \\ 0 & \text{if } x \leqslant 0 \end{array} \right\}. \tag{2}$$

It is simple to verify that for each Boolean threshold function the weights and the threshold value are not unique, however, the sign of each coefficient w_{ij} is uniquely determined (Goles and Martínez, 1991). Thus, if the sign of w_{ij} is positive, then the activation of the element associated to variable j allows the activation of the element associated to variable i, and the opposite, otherwise. The elements of the network and their interactions as defined by their activation functions constitute the *interaction graph*.

The dynamical behavior of the network depends on the type of iteration or updating schedule; parallel and sequential iteration or combinations of them are commonly used. In the first case, the element values are updated at the same time, while in the second case they are updated one by one in a prescribed periodic order. Since it is well known that the set of fixed points of the network is exactly the same for both synchronous and asynchronous iteration (Goles and Martínez, 1991), we decided to apply the synchronous iteration to our dynamical analysis. Thus, the state of the element i on the time $t+1$ is given by $x_i(t+1) = f_i(x(t))$, which means that x_i becomes active if the sum of the input values of f_i, pondered by the weights w_{ij}, is superior than the threshold value θ_i, and inactive otherwise.

Since the number of elements within the network (n) restricts the number of network configurations (2^n), the final state of consecutive iterations is an attractor. An attractor can be a configuration x in $\{0,1\}^n$, called fixed point, that remains stable after a complete iteration, i.e. $x(t+1) = x(t)$, or a set of configurations that may appear periodically as the result of successive iterations, called dynamical cycle. Such attractors can be identified within the different cell types of an organism (Kauffman, 1993; Zuckerkandl, 1994; Huang, 1999). Therefore, a modification or change or perturbation of the genetic regulatory network permits to transit from one attractor to another, for example, from wild type to mutant cell types. In this way, each cellular type is associated to a unique attractor of the regulatory network describing active and inactive genes of the cell network (Kauffman, 1969, 1993).

1.2. Drosophila gastrulation and VF formation

The first visible sign of differentiation in metazoan development is the formation of the germ layers during gastrulation. In *Drosophila*, gastrulation occurs approximately 3 h after fertilization (Costa et al., 1993), during this stage a series of morphogenetic events take place in the embryo: the VF invaginates first and forms the mesoderm and part of the anterior endoderm primordium. At the same time, cephalic furrow is formed on each lateroventral side of the embryo, near its anterior end. Then, at the posterior pole of the embryo, midgut and hindgut primordia invaginate, internalizing the cells that will become the posterior endoderm. Simultaneously, the region of the posterior pole along with the pole cells shift dorsally, beginning the process of germ band extension. During the initial phase of germ band extension, the dorsal epithelium is compressed and forms two deep transverse furrows, which flatten into the amnioserosa at later stages. Cells that remain on the surface of the embryo constitute the ectoderm. They will form mainly epidermis and neural tissue, while the endodermal cells will give rise to the midgut and its

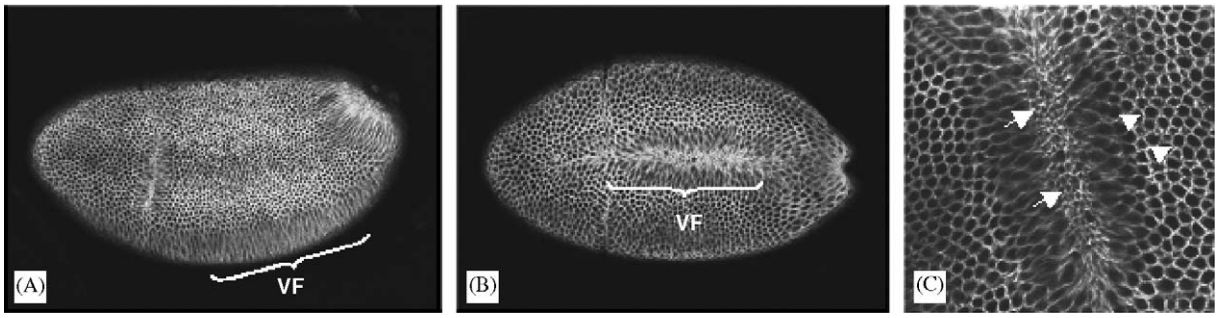

Fig. 1. Confocal images of whole mounts of embryos stained with anti-α-tubulin antibodies: (A) Lateral view of a stage 6–7 embryo (according to Campos-Ortega and Harstenstein, 1985) during gastrulation step, with anterior to the left and dorsal uppermost. Bracket indicates the cells that form the ventral furrow (VF). (B) Ventral view of a similar stage embryo, oriented with anterior to the left, revealing the band of cells along the midventral surface of the embryo that are engaged in VF formation (bracket). (C) Higher magnification view of the ventral region of the same embryo, showing the midventral cells during VF invagination (arrows) and peripheral cells (arrowhead).

appendages, and the mesoderm generates muscle, fat body and gonads.

The formation of the VF is a well-studied process of *Drosophila* gastrulation, mainly because ventral cells begins morphogenetic movements earlier than other regions in the embryo, and they give rise to a conspicuous structure, which is shown in Fig. 1 (Leptin and Grunewald, 1990; Sweeton et al., 1991). VF arises from approximately 20-cells wide band along the midventral surface of the embryo (Fig. 1). This band can be divided in two populations: A central population 8–10 cells wide, and a peripheral population 4–5 cells wide on each side of the central band (Kam et al., 1991). Detailed observations using scanning electron microscopy and epi-illumination video microscopy have revealed the morphological changes that take place in the cells during VF formation (Leptin and Grunewald, 1990; Sweeton et al., 1991). Initially, the central cells undergo apical flattening, and their nuclei move basally increasing cell length along their apical/basal axis (Kam et al., 1991). Some cells begin to reduce their apical diameter, and once the apices of these cells constrict, membranous blebs or ruffles can be observed on their surfaces, suggesting that the contraction of the apical actin cytoskeleton may play a major role in generating the forces for cell shape changes. In agreement with this view, both myosin and β_{HEAVY}-spectrin become localized at the cell apices as soon as apical constriction begins (Kiehart, 1990; Young et al., 1991). When approximately 40% of the central cells have constricted their apices, a rapid transition phase takes place, and the remaining cells, in the ventral domain, begins apical constriction, giving rise to a shallow furrow. The cells start to shorten and widen basally, this change accentuates the wedge-like shape of each cell due to the increased size of the basal surface relative to the constricted apex, and appears to generate the force that drives VF invagination. The peripheral cells do not undergo these shape changes; instead, their apical sides are stretched towards the furrow, suggesting that they are passively drawn into the furrow (Kam et al., 1991).

2. Molecular basis of the model

Given that the shape changes that take place during VF formation are driven by the re-organization of the actin cytoskeleton, the understanding of VF formation requires an assessment of the interplay between upstream regulation and cytoskeletal dynamics. With this in mind we have focused our analysis on gene products that act as transcriptional regulators to specify mesodermal fates, as well as those that function as mediators of the actin cytoskeleton reorganization in a single cell that has been committed to changing its shape. These gene products have been classified according to their cellular roles as: transcription regulatory factors, signaling pathway elements, actin cytoskeletal regulators and regulators of actomyosin network contraction. For some of them, evidences for their involvement in the cell shape changes during VF invagination came from phenotypic analysis of mutant *Drosophila* embryos. For the others, evidences of biochemical and cell biology studies in *Drosophila* and *Caenorhabditis elegans* and studies in cell culture models provide support for their putative role in the cell shape changes described here.

2.1. Transcription factors controlling VF formation

A signaling cascade that activates the transmembrane receptor Toll on the ventral side of the embryo specifies VF cells. Toll signaling results in the dissociation of the cytoplasmic heterodimer of Dorsal and Cactus; free Dorsal migrates into the nuclei of ventral cell where it activates the transcription of *twist* (*twi*), a basic helix-loop-helix protein (Jiang et al., 1991) and *snail* (*sna*), which encodes a zinc-finger transcriptional regulator (Boulay et al., 1987). Twi and Dorsal act cooperatively

to further activate the ventral expression of *sna* in a domain that coincides with the limits of the presumptive mesoderm. Since Twi and Dorsal act synergistically to activate *sna,* in *twi* mutants, *sna* is still expressed normally in a narrow domain of 8–10 cells wide along the ventral midline (Leptin, 1991). Previous studies indicate that *twi* and *sna* are required for VF formation and mesoderm differentiation, as both processes are disrupted in each mutant. However, they have distinct roles during embryogenesis, while Twi has been implicated as an activator of mesordermal genes, Sna is known to function as a repressor of neuroectodermal genes (Kosman et al., 1991; Leptin, 1991; Hemavathy et al., 1997). Moreover, several lines of evidence suggest that *twi* and *sna* also have different effects on the cell shape changes that occur during VF formation (reviewed in Leptin, 1995), since mutations in either of these genes differentially affect the cell phenotypes i.e. nuclear movement, apical constriction and shortening, as discussed in Section 3.3.

2.2. Signaling pathway elements

Two genes, *fog* and *cta*, specifically affect VF formation; *fog* is a transcriptional target of Twi and Sna and encodes a zygotically acting putative secreted protein, which is expressed locally in the VF cells (Costa et al., 1994). In contrast to *fog*, *cta*, which encodes a putative G-protein α-subunit, is maternally supplied and *cta* mRNAs are distributed ubiquitously throughout the embryo (Parks and Wieschaus, 1991). Cta protein is only 35–44% identical to previously characterized *Drosophila* Gα subunits, however it is more similar to mouse proteins Gα-12 and Gα-13 subunits (Parks and Wieschaus, 1991). Mutations in both genes result in practically identical phenotypes, which are significantly less severe than *twi* or *sna* mutants. In embryos lacking *fog* or *cta* activity, the induction of cell shape changes is delayed and the coordination of the invagination process is disrupted, however the mesoderm is eventually internalized (Parks and Wieschaus, 1991; Costa et al., 1994). Due to the non-essential function of *fog* and *cta*, they have been implicated in the coordination, rather than the control of cell shape changes during VF formation (Costa et al. 1994).

The close resemblance of the phenotypes caused by *fog* and *cta* mutations, and the fact that both genes encode putative signaling molecules, has led to propose a model that places both genes in a common signal transduction pathway. In this model Fog binds to an unidentified receptor triggering Cta activation (Costa et al., 1994). In order to test this model, the ectopic expression of *fog* using an inducible promotor and the constitutive activation of *cta* has been examined (Morize et al., 1998). Uniform activation of *fog* and *cta* is not lethal, but results in ectopic cell shape changes in the gastrula. Ectopic expression of *fog* does not rescue the gastrulation defects of *cta* mutant embryos, indicating that Cta is required for the cell shape changes induced by Fog and thus may be acting downstream from *fog* in wild-type embryos (Morize et al., 1998).

2.3. Actin cytoskeleton regulators

In *Drosophila*, embryos lacking the gene RhoGEF2, which encodes a putative GEF for Rho, fail to gastrulate due to defects in the cell shape changes required for VF formation, indicating that RhoGEF2 is a critical signaling component for gastrulation (Barrett et al., 1997; Häcker and Perrimon, 1998). The evidences that RhoGEFs may be activated through their interactions with Gα-12/13 subunits (Hart et al., 1998; Kozasa et al., 1998; Yau et al., 2003) raised the idea that *Drosophila* VF formation may be triggered by the Fog/Cta pathway activating RhoGEF2. Furthermore, a regulator of G protein signaling domain that is highly homologous to that of mammalian RGS–RhoGEFs was identified at the N-terminus of RhoGEF2 (Kozasa et al., 1998). These results led to the conclusion that the Gα-12/13–RhoGEF–Rho pathway has been highly conserved during evolution. However, these observations are not consistent with the phenotypes of the *Drosophila* mutants; RhoGEF is essential for cell shape changes during VF formation, while Fog/Cta are only involved in coordinating or accelerating these changes (Häcker and Perrimon, 1998).

The predicted cellular role of GAPs as inhibitors of small GTPases has been supported by several in vivo studies (see Gaul et al., 1992). In our model, excess accumulation of GTP-Rho due to a defect in GTP hydrolysis might cause non-physiological activation of the Rho effectors, interfering with proper cell shape changes. We proposed that RhoGAP is activated by Src-mediated phosphorylation, based on the results of Brouns et al. (2001). Upstream Src we have placed the G-protein α-subunit, *cta*, working through the tyrosine kinase Csk (C-terminal Src kinase) to Src kinase to GAP in order to relieve the suppression on Rho activity. Evidence of a Gα mediated actin reorganization come from a recent study of Lowry et al. (2002) showing that Csk is critical for relaying G protein signals to actin cytoskeleton in mammalian culture cells. Csk negatively regulates the activity of Src through the phosphorylation of the tyrosine residue of its C-terminal tail (Okada et al., 1991). Csk is ubiquitously expressed in mammalian cells and is evolutionarily conserved from Hydra to humans (Miller et al., 2000). In *Drosophila,* the ortholog of the mammalian Csk has been identified as the gene CG17309 (Morrison et al., 2000). Therefore, it is possible to suggest that heterotrimeric Gα-12/13 proteins may control the activity of Rho by increasing the activity of the positive regulator RhoGEF and/or by

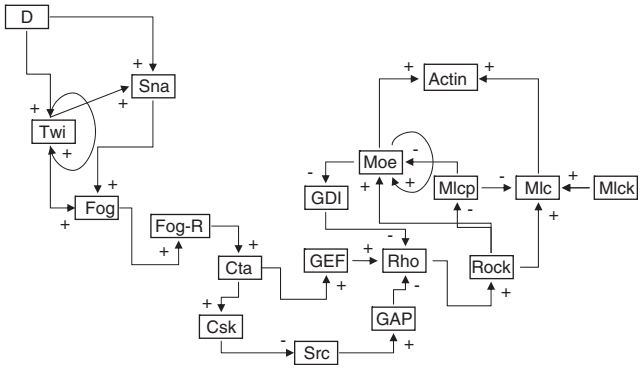

Fig. 2. Genetic regulatory network for *Drosophila* VF formation constructed from published genetic and molecular data. Abbreviations are as follows: (D) Dorsal; (Twi) twist (Sna) snail; (Fog) Folded-gastrulation; (Fog-R) Fog receptor; (Cta) Concertina; (GEF) Rho Guanine-exchange factor 2 or RhoGEF2; (Csk) C-terminal Src kinase; (Src) Src kinase; (GAP) GTPase-activating protein; (Rock) Rho-kinase; (GDI) Guanine nucleotide dissociation inhibitors; (Moe) Moesin; (Mlcp) Myosin light chain phosphatase; (Mlck) Myosin light chain kinase (Mlc) Myosin light chain.

decreasing the activity of the negative regulator Rho-GAP as described in our model (Fig. 2).

In resting cells, Rho GTPase exists mostly in the GDP-bound form and in complexes with Rho-GDI in the cytosol (Sasaki and Takai, 1998). The release of Rho-GDI from Rho is necessary before Rho becomes susceptible to GEF activity (Kikuchi et al., 1992; Kuroda et al., 1992). Biochemical analysis suggests that binding of Rho-GDI to ERM (Hirao et al., 1996), a member of ezrin, radixin, and moesin family of proteins, help to dissociate it from GDP · Rho (Takahashi et al., 1997). ERM proteins bind F-actin and contribute to the organization of cortical actin filaments after being activated through phosphorylation of their C-terminal residues (Tsukita and Yonemura, 1999). Although, activation of ERM seems to be a prerequisite for the activation of the Rho signaling pathway, Rho is able to generate the active conformation of ERM proteins, through its downstream target Rho-kinase (Matsui et al., 1998; Simons et al., 1998). Since the phosphorylation state of Moesin seems to be regulated by the activity of both Rho-kinase and myosin light chain phosphatase (MLCP) (Fukata et al., 1998) a positive feedback cycle that amplifies the signal transduction pathway by activating ERM proteins can be predicted as depicted in the interaction graph of Fig. 2.

2.4. Regulators of actomyosin network contraction

Several lines of evidence indicate that Rho GTPases are signal transducers upstream from actin cytoskeleton rearrangements and myosin regulation (Van Aelst and Symons, 2002). In *Drosophila*, injection of mutant forms of Rho or Cdc42 proteins alters the actomyosin cytoskeleton, disrupting the process of cellularization (Crawford et al., 1998). At later stages of embryogenesis, expression of a dominant negative form of Rac1 and Cdc42 disrupt the actomyosin cytoskeleton at the leading edge cells during dorsal closure (Harden et al., 1995). As mentioned before, the embryos that lack maternal RhoGEF2 fail during apical constriction of VF cells. Interestingly, myosin localizes to the apical ends of these VF cells (Young et al., 1991). This observation coupled with the genetic interaction between RhoGEF2 and myosin during *Drosophila* leg morphogenesis (Halsell et al., 2000) suggests that RhoGEF2 may exert some of its effect during VF formation via the activity of myosin in the VF cells.

Rho GTPase may control the activity of smooth muscle and non-muscle myosin II by regulating the phosphorylation state of the myosin regulatory light chain (MLC, reviewed in Somlyo and Somlyo, 2003), which in turn is modulated by the antagonistic activity of myosin light chain kinase (MLCK) and MLCP. In vitro assays revealed that Rho-kinase phosphorylates MLC and induces the activity of myosin (Amano et al., 1996; Kureishi et al., 1997). Moreover, Rho-kinase can phosphorylate the myosin binding subunit of MLCP, decreasing its activity, which results in the accumulation of phosphorylated MLC and a contractile response (Kimura et al., 1996). In *Drosophila*, the regulation of the phosphorylation state of myosin regulatory light chain seems to be essential for myosin II functions during many developmental processes (Winter et al., 2001; Mizuno et al., 2002; Tan et al., 2003).

The ability of Rho-kinase to positively regulate myosin II activity suggests that activated Rho can mediate cell shape changes through this downstream effector by modulating the contractile state of the actomyosin network (Fig. 2). A similar model has been proposed to explain elongation of the *C. elegans* embryo, which is due to actin-mediated contractions within the lateral epidermal cells (Priess and Hirsh, 1986). Genetic screens in *C. elegans* have identified mutations in loci encoding Rho signal transduction components (Wissmann et al., 1997). The pathway that regulates elongation includes: LET-502/ROK and MEL-11/MLCP. MEL-11 prevents contraction by dephosphorylating MLC-4/MLC. In turn, LET-502 inhibits MEL-11, releasing the block to elongation (Piekny et al., 2000; Piekny and Mains, 2002; Wissmann et al., 1999).

3. Implementation of the model

We used published genetic and molecular data to define the activity of 18 genes during the cell shape changes that characterize VF formation. We proposed a simple mathematical model to understand the global and emergent dynamical behavior of a network, in

which the information flows from transcriptional regulators through cascades of intracellular signaling, which in turn, modulate the organization of the actin cytoskeleton. In this model, we combined several biochemical processes such as transcriptional activation, ligand binding, protein modification, etc. We intended to recognize whether the previous knowledge about the components of this network is sufficient to describe wild type and mutant cell types during VF formation.

In our model, we assumed that individual cells behave independently of each other within the ventral epithelium. Moreover, the cell represented in our model corresponds to a central cell as defined by Leptin and Grunewald (1990), which initiates the cell shape changes at the onset of VF formation. Previous evidence indicates that the behavior of individual cells within the ventral epithelium seems to be independent of one another: Ventral cells initiate constriction in a stochastic manner (Kam et al., 1991; Sweeton et al., 1991) that appears to be more consistent with cell autonomy than with coordination by cell–cell interactions. Support for cell autonomy during VF formation comes from mosaic studies showing that wild type cells within an environment of mutant non-constricting cells are able to constrict and invaginate. Thus, the cooperative activity of ventral cells is not required to allow invagination, suggesting that the cell shape changes themselves generate the force for VF formation (Leptin and Roth, 1994).

Even though the activation rates of the different network elements describing the cell shape changes could not be distinguished, we knew whether or not each element was active or inactive at a certain interval of time and decided to use a Boolean logical model. In this model, each element of the regulatory network (ie. the gene products of *sna*, *twit*, etc.) was associated to a Boolean variable (x_{Sna}, x_{Twi}, etc.), where 1 indicates that the element is activated and 0 indicates otherwise. The activation states for each element in the network are defined as follows:

1. Dorsal (D) = transcriptional activation of *twi* and *sna*.
2. Twist (Twi) = transcriptional activation of Twi target genes.
3. Snail (Sna) = transcriptional activation/repression of Sna target genes.
4. Folded-gastrulation (Fog) = binding to Fog receptor (Fog-R).
5. Receptor (Fog-R) activated = Signal transduction trough Cta.
6. Concertina (Cta) = activation of RhoGEF2 and Csk kinase.
7. Rho Guanine-exchange factor 2 (RhoGEF2) = activation of Rho.
8. C-terminal Src kinase (Csk) = inactivation of Src kinase.
9. Src kinase = activation of Rho-GAP.
10. GTPase-activating proteins (GAP) = inactivation of Rho.
11. Rho = activation of Rock.
12. Rho-kinase (Rock) = activation of Moesin and Mlcp.
13. Guanine nucleotide dissociation inhibitors (GDI) = sequestering/inactivation of Rho.
14. Moesin (Moe) = inactivation of GDI, actin reorganization.
15. Mlcp = inactivation of myosin.
16. Mlck = activation of myosin.
17. Myosin (Mlc) = reorganization of actin into an actomyosin contractile network.
18. Actin = cytoskeletal re-organization.

As a result, $x = (x_D, x_{Twi}, \ldots, x_{Actin})$ in $\{0,1\}^{18}$ represents the state vector that at a given time indicates the activity of the 18 elements that conform the regulatory network.

The information that defines the activation functions of each element in the regulatory network is shown in Table 1. For the mesodermal transcriptional regulators, their direct interactions were derived from mutant phenotypes affecting VF formation (summarized in 2.1). Similar evidences were used to define the activity of the Fog/Cta signal transduction pathway. However, in this case we assumed the existence of a G protein-coupled receptor, which is activated upon the binding of Fog to affect Rho-mediated signaling throughout the activity of Cta (summarized in 2.2). A set of interactions that link Rho-GEF, Rho-GAP and Rho-GDI with their regulators was derived from results obtained with

Table 1
Activation function of each element of the network

$f_D = 1$ (cte)	$f_{GEF} = x_{Cta}$	$f_{GDI} = \sim x_{Moe}$
$f_{Twi} = OR^{a}(x_{Twi}, x_D)$	$f_{Csk} = x_{Cta}$	$f_{Moe} = \mathrm{AND}(x_{rock}, x_{mlcp}, x_{Moe})^{b}$
$f_{Sna} = x_D$	$f_{Src} = \sim x_{Cta}$	$f_{mlcp} = \sim x_{rock}$
$f_{Fog} = OR^{a}(x_{Twi}, x_{Sna})$	$f_{GAP} = OR^{a}(x_{Scr}, x_{GAP})$	$f_{mlck} = 1$ (cte)
$f_R = x_{Fog}$	$f_{Rho} = AND^{b}(\sim x_{GDI}, x_{GEF}, \sim x_{GAP})$	$f_{mlc} = AND^{b}(\sim x_{mlcp}, x_{rock}, x_{mlck})$
$f_{Cta} = x_R$	$f_{rock} = x_{Rho}$	$f_{\mathrm{Actin}} = AND^{b}(x_{Moe}, x_{mlc})$

[a]OR $(x_1, x_2, \ldots, x_n) = 1$ if and only if there exists i in $\{1, 2, \ldots, n\}$ such that $x_i = 1$. And $\sim x_i = 1$ if and only if $x_i = 0$.
[b]AND$(x_1, x_2, \ldots, x_n) = 1$ if and only if $x_i = 1$ for all $i = 1, \ldots, n$.

mutant *Drosophila* embryos, as in the case of RhoGEF2 or inferred from data obtained with cell culture systems, as in the cases of GAP and GDI (summarized in 2.3). The action of activated Rho on actin contraction was based on genetic and biochemistry studies in *Drosophila* and *C.elegans* (summarized in 2.4).

The function $\mathrm{AND}(x_1, x_2, \ldots, x_n)$ is a threshold function that can be written as: $\mathrm{AND}(x_1, x_2, \ldots, x_n) = H(x_1 + x_2 + \cdots + x_n - n)$, where the function Heaviside H is defined as in Eq. (2) of Section 1.1. Furthermore, we can replace x_i by $\sim x_i$ by changing x_i by $(1-x_i)$ in the argument of the function Heaviside. Thus, $\mathrm{AND}(x_1, \ldots, \sim x_i, \ldots, x_n) = H(x_1 + \cdots + (1 - x_i) + \cdots + x_n - n)$. In the case of the function $\mathrm{OR}(x_1, x_2, \ldots, x_n)$, an analogous observation can be made. Consequently, the activation functions defined in Table 1 are all Boolean threshold functions. Based on this model description, we constructed a first interaction graph of the regulatory network, which is shown in Fig. 2, where the dependence of the activation function of i on the variable j is represented by the arc from j to i, and its sign is equal to the sign of w_{ij} of the threshold representation of the function, which is uniquely determined.

3.1. Dynamics of the network

The central hypothesis of the model predicts that, during VF formation, the wild-type cell is characterized by the three mentioned phenotypes and corresponds to the stable state vector (fixed point) $x^* = (1,1,1,1,1,1,1,1,0,0,1,1,0,1,0,1,1,1)$ of our regulatory network, where all the elements of the network are active except Src, GAP, GDI, and Mlcp, which are inhibited. Furthermore, the network must be robust against mutations; i.e. each mutant cell type should correspond to a stable state of a network that is now modified according to the nature of the mutation.

We can observe that: If $x = (x_D, x_{Twi}, \ldots, x_{Actin})$ in $\{0,1\}^{18}$ is a stable state vector of the network, where $x_D = 1$, then the value for each other variables corresponds exactly to those of x^*, which is in agreement with our hypothesis, except that $(x_{Rho}, x_{Rock}, x_{GDI}, x_{moe}, x_{mlcp}, x_{mlc}, x_{Actin})$ can also take the value (0,0,1, 0,1,0,0). In other words, the regulatory network shown in Fig. 2 has only two fixed points:

I $x^* = (1,1,1,1,1,1,1,1,0,0,1,1,0,1,0,1,1,1)$,

and

II $y^* = (1,1,1,1,1,1,1,1,1,0,0,0,0,1,0,1,1,0,0)$.

Since Actin is inhibited in y^*, and consequently there are not cell shape changes, this vector is not observed in wild-type embryos. Hence, x^* is the only fixed point of the network where Actin is active in wild-type embryos. Furthermore, this vector has a great basin of attraction, indeed, independently of the type of iteration that was used, every vector z in $\{0,1\}^{18}$ where $z_D = z_{mlck} = z_{Moe} = 1$ after of a finite number of iterations converges to the fixed point x^*.

3.2. Relationships between the structure and the dynamics of the network

The number of possible fixed points of a regulatory network is connected to the structure of the interaction graph, in particular, to the positive feedback loops or positive circuits in the interaction graph. The importance of the positive and negative circuits in the multiple equilibriums and homeostasis of a given genetic regulatory network, and particularly in generalized logical networks, has been extensively studied (Thieffry et al., 1995; Thomas et al., 1995). In the case of Boolean threshold networks, Aracena et al. (2002, 2004) and Demongeot et al. (2003) showed that there are a limit for the maximum number of fixed points in terms of the number and interconnections of positive circuits in the connection graph.

Aracena et al. (2002, 2004) proved that the maximum number of fixed points of a Boolean threshold network is $2^{|\tau(G)|}$, where $\tau(G)$ is the minimum set of nodes covering the positive circuits of the interaction graph G, which is not necessarily unique, and $|\tau(G)|$ is the cardinality of the $\tau(G)$. Furthermore, the vector of states of these nodes is different for each fixed point, namely, if $\tau(G) = \{t1, t2, \ldots, tp\}$ and x and y are two distinct fixed points, then the vectors $(x_{t1}, x_{t2}, \ldots, x_{tp})$ and $(y_{t1}, y_{t2}, \ldots, y_{tp})$ are also different. In this way, there is a correspondence between the fixed points of the network and the states of the nodes of $\tau(G)$. In our original network there are five positive circuits in the graph: The self-loop of Twi, Moe and GAP, and the feedback loops: Moe-GDI-Rho-Rock-Moe and Moe-GDI-Rho-Rock-Mlcp-Moe. Consequently, $|\tau(G)| = 3$, where $\tau(G) = \{Twi, Moe, GAP\}$. Hence, the vectors x^* and y^* described in previous section can be only characterized by the state values of the variables x_{Twi}, x_{GAP} and x_{Moe}. Thus, the fixed point x^* can be represented by the vector $(x_{Twi}, x_{GAP}, x_{Moe}) = (1,0,1)$ and y^* by $(x_{Twi}, x_{GAP}, x_{Moe}) = (1,0,0)$. This means that the value of the vector $(x_{Twi}, x_{GAP}, x_{Moe})$ determines the state values of the rest of the element at each stable state of the network. Moreover, in the wild type cell the only positive circuits of the network with different state configurations for each stable state are those including the element Moe.

3.3. Robustness of the regulatory network

An alternative to test the robustness and consistency of the regulatory network proposed in Fig. 2 is the analysis of the effects of mutations (Sánchez et al., 1997;

Sánchez and Thieffry, 2001, 2003; Albert and Othmer, 2003). By doing so, we will also be able to determine the main components of the network that are responsible for the occurrence of each of the three phenotypes under study. The mutations analysed in this work are loss-of-function mutations, which can be simulated by assigning the value zero to the corresponding variable and logical function.

A simulation of a loss-of-function mutation of *cta* or *fog* genes in the network of Fig. 2 results in a network having stable state with $x_{GEF} = 0$. The result is in disagreement with the experimental information on these mutants, since the modification of the wild-type cell observed in *RhoGEF2* mutant embryos is different from that of *cta* or *fog*. In fact, *RhoGEF2* loss-of-function mutations result in midventral cells capable of undergoing nuclei release from the apical side, but unable to constrict their apices and shorten their length (Häcker and Perrimon, 1998; Barrett et al., 1997). *RhoGEF2* mutant embryos fail to gastrulate indicating the critical role of *RhoGEF2* in the cell shape changes required for VF formation. On the other hand, *fog* and *cta* mutant embryos still constrict their VF cells and internalize the mesoderm even though shape changes are delayed and uncoordinated (Costa et al., 1994; Sweeton et al., 1991). The observations of these mutant cell phenotypes have led to propose the existence of at least one additional activator of *RhoGEF2* (Häcker and Perrimon, 1998), this element in the network, named as A, represents the so-called zygotic initiator of apical constriction (Costa et al., 1994; Häcker and Perrimon, 1998; Leptin, 1999). Given that embryos with half of *twi* doses show several minutes delay in VF formation (Leptin and Roth, 1994), it is possible that the level of A is limiting and that this component needs to accumulate until reaching a critical level required for shape changes. Considering this, we have represented this functional dependence of A by a loop. Since we know that the cell types observed in both *twi* and *RhoGEF2* mutant embryos exhibit similar phenotypes (see below), we connected them in a common pathway through A. The logical activation function assigned to A is equal to $f_A = OR(x_{Twi}, x_A)$, therefore, the activation function of *RhoGEF2* is redefined by $f_{GEF} = OR(x_{Cta}, x_A)$.

As mentioned before, the three phenotypes that depict the cell shape changes during VF formation involve actin cytoskeletal re-organization. In terms of the modeling, this means that a cell exhibiting any of the three phenotypes must be associated to a stable vector x, whose variable x_{Actin} has the value 1. The phenotype predicted from a simulation of loss-of-function mutation of *twi* in the network reveals that if x is a stable state of the network, then $x_{Rho} = 0$ and consequently $x_{actin} = 0$, which is in disagreement with the observation that in *twi* mutants a transient VF of abnormal appearance still forms in a stripe 8–10 cells wide that probably corresponds to the expression domain of *sna*. These cells undergo some of their characteristics shape changes: Nucleus movement from apical to basal side and increasing in cell length along the apicobasal axis (Costa et al., 1993; Leptin and Grunewald, 1990). Here we proposed that these cell shape changes are under *sna* control, represented by a connection to a new element named as B. Moreover, we hypothesize that B might corresponds to a second signaling cascade involving the small GTPase Rap1 (as discussed in Section 4). The added element B connects Snail to Actin, with the activation function $f_B = x_{Sna}$ and the activation function of Actin is then redefined by $f_{Actin} = \mathrm{OR}(x_B, AND(x_{Moe}, x_{Mlc}))$, which can be written as $f_{Actin} = H(2x_B + x_{Moe} + x_{Mlc} - 2)$, i.e. f_{Actin} is also a Boolean Threshold function.

Therefore, we suggest a new regulatory network with 20 elements controlling the cell shape changes in VF, whose interaction graph is shown in Fig. 3. The vector x' in $\{0,1\}^{20}$ defined by $x' = (x^*, x_A = 1, x_B = 1)$ where y^* in $\{0,1\}^{18}$, which is the vector associated to the wild type cell defined previously in Section 3.1, is an stable state of the new network with a big basin of attraction in agreement with the hypothesis of the model. The another stable state of this network: $y' = (y^*, y_A = 1, y_B = 1)$ where y^* in $\{0,1\}^{18}$ was defined in Section 3.1.

The robustness and consistency of the new regulatory network shown in Fig. 3 was also tested by simulation and analysis of loss-of-function mutations. To simplify the analysis we studied the state values of a group of ten elements: Twist, Sna, Fog, Cta, RhoGEF2, GAP, Rho, Actin, A and B, among the 20 elements of the network. We selected these elements based on one hand in the existence of well-characterized mutations and on an-

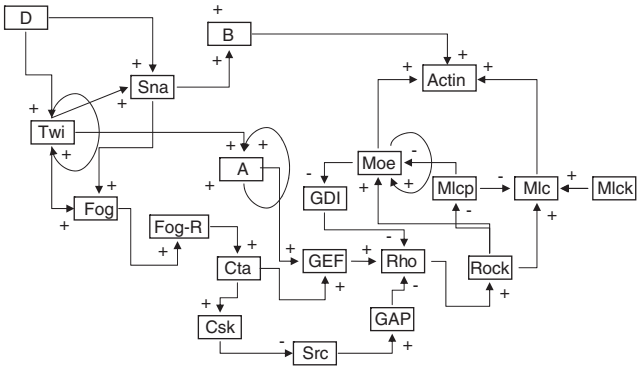

Fig. 3. Genetic regulatory network proposed for *Drosophila* ventral furrow formation with the minimal structure to satisfy the model requirements. Abbreviations are as follows: (D) Dorsal; (Twi) twist (Sna) snail; (Fog) Folded-gastrulation; (Fog-R) Fog receptor; (Cta) Concertina; (GEF) Rho Guanine-exchange factor 2 or RhoGEF2; (Csk) C-terminal Src kinase; (Src) Src kinase; (GAP) GTPase-activating protein; (Rock) Rho-kinase; (GDI) Guanine nucleotide dissociation inhibitors; (Moe) Moesin; (Mlcp) Myosin light chain phosphatase; (Mlck) Myosin light chain kinase (Mlc) Myosin light chain.

other in the fact that for a given stable state of the network the state values of these elements allow to determine the state values of the rest. For example, let x in $\{0,1\}^{20}$ be a stable state vector of the network, if $x_{Rho} = 1$, then $(x_{Rock}, x_{GDI}, x_{moe}, x_{mlcp}, x_{mlc}, x_{Actin}) = (1,0,1,0,1,1)$ and $(x_{Rock}, x_{GDI}, x_{moe}, x_{mlcp}, x_{mlc}, x_{Actin}) = (0,1,0,1,0,0)$ otherwise. This stable state vector corresponds to the values of the vector (x_{Twist}, x_{Sna}, x_{Fog}, x_{Cta}, x_{GEF}, x_{GAP}, x_{Rho}, x_{Actin}, x_A, x_B). Besides, a phenotypic vector $p = (p_{NM}, p_{AC}, p_{CS})$ in $\{-1,1\}^3$ is associated to the cellular phenotypes observed in wild type or mutant cells, where $p_{NM} = 1$, if there is nuclear movement in the cell and 0 otherwise; $p_{AC} = 1$, if there is apical constriction in the cell and 0 otherwise; and $p_{CS} = 1$, if there is cell shortening in the cell and 0 otherwise. Thus, the phenotypic vector associated to the wild type cell is $p = (1,1,1)$. The following section discussed the phenotypes predicted from the simulation of loss-of function mutations in the above-mentioned genes. Table 2 presents a summary of the mutations, stable states and associated phenotypic vectors.

3.3.1. Simulation of loss-of-function mutants

Loss-of-function sna mutation: This mutant cell type has the associated phenotypic vector $p = (-1,-1,1)$, i.e. only cell shortening is observed in the cell. The network reaches only one stable state where Actin is active: (1,0,0,0,1,0,1,1,1,0). In this case $x_{Rho} = 1$ and $x_B = 0$, therefore, Actin is activated through the pathway Twist → A → RhoGEF2 → Rho, which might control cell shortening in agreement with the observation of mutant phenotypes. The evidence indicates that the nuclei of *sna* mutant cells remain close to the apical side while cells become shorter and more cuboidal (Leptin and Grunewald, 1990), suggesting that cell shortening is under the control of Twi. Moreover, analyses of RhoGEF2 mutations indicate that cell shortening does not occur in these mutant cells, suggesting that Twi acts through RhoGEF2 to activate this change in the cellular shape.

Loss-of-function twi mutation: The network reaches two stable states: (0,1,0,0,0,1,0,1,0,1) and (0,1,0,0,0,0,0,1,0,1). In both cases $x_{GEF} = x_{RHO} = 0$ and consequently Actin is activated only through of the pathway Snail → B. The only difference between them is the value of x_{GAP}, which in this case can adopt two possible values. This result probably indicates the existence of several regulators of GAPs. GAPs are large molecules containing multiple domains in addition to their GAP catalytic domain, such as SH2, SH3, proline-rich, and GTPase domains, indicating that they are likely to interact with additional proteins. GAPs may also be regulated by phosphorylation, for example p190 RhoGAP, a GTPase-activating protein for Rho is phosphorylated and activated by the tyrosine kinase Src (Brouns et al., 2001) leading to the inhibition of Rho activity (Chang et al., 1995; Arthur et al., 2000). In this case, the associated phenotypic vector is $p = (-1,1,-1)$, i.e. there is only nuclear movement. This result is in agreement with the observation that in the absence of Twi, *sna* will still be expressed in a narrower midventral domain (Leptin, 1991), however inputs from Twist over *fog* and A are missed, thus only basal movement of the nuclei is observed in a stripe 8–10 cells wide along the ventral midline (Leptin and Grunewald, 1990; Costa et al., 1993).

Double loss-of-function twi-sna mutation: The network has two stable states (0,0,0,0,0,0,0,0,0,0) and (0,0,0,0,0,1,0,0,0,0). In both cases the only variable with a value different to zero is x_{GAP}. Since Src is activated, the final activation of GAP depends on itself. However, in both

Table 2
Results of simulations of loss-of-function mutants

Genetic background	Stable states[a] (x_{Twist}, x_{Sna}, x_{Fog}, x_{Cta}, x_{GEF}, x_{GAP}, x_{Rho}, x_{Actin}, x_A, x_B)	Phenotypic vector $p = (p_{NM}, p_{AC}, p_{CS})$	Comment on phenotype[b] perturbations
Wild type	(1,1,1,1,1,0,1,1,1,1)	(1,1,1)	
Loss-of-function *sna*	(1,0,0,0,1,0,1,1,1,0)[a]	(−1,−1,1)	Cell nuclei remain close to the apical surface, VF cell shorten along its apico-basal axis
Loss-of-function *twi*	(0,1,0,0,0,0,0,1,0,1)[a]	(−1,1,−1)	Basal movement of the nuclei is observed, apical surfaces of the cell does not constrict, cell does not shorten
	(0,1,0,0,0,1,0,1,0,1)[a]		
Loss-of-function *twi/sna*	(0,0,0,0,0,0,0,0,0,0) (0,0,0,0,0,1,0,0,0,0)	(−1,−1,−1)	The three cell phenotypes are perturbed
Loss-of-function *cta*	(1,1,1,0,1,0,1,1,1,1)	(1,1,1)	The three cell phenotypes are observed
Loss-of-function *fog*	(1,1,0,0,1,0,1,1,1,1)	(1,1,1)	The three cell phenotypes are observed
Loss-of-function *RhoGEF2*	(1,1,1,1,0,0,0,0,1,1)	(−1,1,−1)	Same as described for loss-of-function *twi* mutation

[a]Only stable states where Actin is activated were considered.
[b]Phenotypes that describe the cell shape changes of wild type or mutant cells during VF invagination: Apico-basal nuclear movement, apical constriction and cell shortening.

cases Actin is not activated and therefore there are not changes in the shape of this mutant cell type. This is coherent with the experimentally observed phenotypic vector $p = (-1, -1, -1)$. Based on this result, we suggest that apical cell constriction is due to the combined action of Snail, Twist and RhoGEF2.

Loss-of-function fog or cta mutation: The cell type observed in *fog* and in *cta* mutants is practically identical. In both cases, the associated phenotypic vector is the same $p = (1, 1, 1)$ and it is also the same for wild type cells. In the case of the *fog* mutation the stable state with Actin activated is (1,1,0,0,1,0,1,1,1,1) and in the case of *cta* mutation is (1,1,1,0,1,0,1,1,1,1), i.e. the only difference is the state value of x_{Fog}. Beside, in both cases Actin is activated trough the pathways: Snail → B and Twist → A → RhoGEF2 → Rho, which fits the observation that, in *fog* and *cta* mutations the three phenotypes that describe cell shape changes during VF formation are still observed (Parks and Wieschaus, 1991; Costa et al., 1994). In addition, this result shows the robustness of the constructed network against the analysed mutations.

Loss-of-function RhoGEF2 mutation: The network reaches only one stable state: (1,1,1,1,0,0, 0,0,1,1). In this case, the phenotypic vector associated is $p = (-1, 1, -1)$, i.e. there is only nuclear movement, as in *twi* mutation, since Actin is activated through the pathway Snail → B. Accordingly, nuclear movement is the only phenotype observed in RhoGEF2 mutant cell type as reported by Barrett et al. (1997) and Häcker and Perrimon (1998).

4. Discussion

In this work, our main goal was to explore whether the molecular data available could be combined in a dynamic model compatible with the cell shape changes that take place during VF formation. Due to the lack of quantity data about the activity of the elements of the network we selected a Boolean network as the dynamical model.

The Boolean networks have been commonly used to model genetic regulatory networks due to the simplicity of its formulation and computation (see, for example, Bodnar, 1997; Mendoza and Alvarez-Buylla, 1998; Sánchez and Thieffry, 2003). Moreover, the comparisons between the mathematical results on the dynamical properties of this type of network and the use of differential equation to model genetic regulatory networks (Snoussi and Thomas, 1993; Thomas et al., 1995) provide the confidence that the Boolean networks are useful to study quality properties of the dynamical behavior of gene interaction. Discrete modeling of *Drosophila* regulatory networks has been the focus of several reports (Sánchez and Thieffry, 2003; Sánchez and Thieffry, 2001; Sánchez et al., 1997; Albert and Othmer, 2003). One main point that distinguished those works with the one presented here is the suggestion of missed elements and connections such that the proposed network results to be coherent with the qualitative information obtained from wild type and mutant cells. Besides, we attempted to understand which combination(s) of the elements within the network controls each of the three phenotypes that describe cell shape changes during VF formation. As a result of the analysis of the regulatory network robustness, we can propose the existence of at least two new elements and a positive feedback loop, and suggest how they may be connected to the other elements of the network. Moreover, since the dynamical behavior of the network was centered in the steady states of the system, the results that we obtained are valuables for different types of iteration.

The biological information on the network presented here indicates the existence of a general cellular machinery that is able to produce the cell shape changes. This machinery is formed by several elements with ubiquitous expression in the embryo, among them Cta, RhoGEF2, Myosin and Actin, which are maternally supplied and whose expression can be detected in all the cells of the embryos. Therefore, in order to generate the specific cell shape changes observed at the VF cells, the expression of some of the components must be temporal and/or spatially regulated. Fog is one of these components; it is expressed transiently and exclusively in the cells that form the VF, however biological evidence indicates that its activity is insufficient to explain the behavior of the ventral cells during VF formation (Costa et al., 1994). Therefore, we proposed the existence of elements A and B, and linked them with the rest of the elements in the network based on biological information, in particular, phenotypic analysis of mutant embryos.

During VF formation the earlier cells constricting their apices are localized to the central region of the furrow, as does the cell represented in our model, and they do not require the expression of *fog* to initiate constriction. Mutation analyses reveal that apical constriction of the central cell is neither seen in *twi* nor in *sna* mutants (Leptin and Grunewald, 1990), therefore we assumed that both transcriptional regulators are needed to elicit this shape change. Furthermore, the apical constriction is not observed in RhoGEF2 mutants either, revealing the essential role of RhoGEF2 during VF formation, as a regulator of a signaling cascade involving the Rho GTPase (Barrett et al., 1997; Häcker and Perrimon, 1998). The central cells reach threshold levels of *twi* and *sna* (Leptin and Roth, 1994) more rapidly than peripheral cells, and thus they might be able to activate the early transcription of the zygotic initiator, represented here by A, which induce constriction in a cell-autonomous manner. At the same time, the

transcription of *fog* is activated in the central cells, as evidenced by in situ staining of *fog* transcripts (Costa et al., 1994). As a result, secreted Fog will signal the neighbor cells, and might reinforce apical constriction through further activation of RhoGEF2. In this scenario the product of *fog* gene seems to function in a non-autonomous manner after the cells have initiated their apical constrictions, and thus it is assumed that Fog accelerates this process in the remaining cells of the ventral region. This supposition seems to be consistent with the phenotypes of *fog* and *cta* mutants (Parks and Wieschaus, 1991; Costa et al., 1994). In these mutant embryos, the cell shape changes occur more slowly and in a less orderly fashion than in wild-type embryos. However, the ventral cells retain the capacity to constrict, a furrow is eventually formed and the mesoderm develops normally (Parks and Wieschaus, 1991; Sweeton et al., 1991; Costa et al., 1994).

When loss-of-function *twi* mutants are observed, two cell phenotypes appears altered, apical constriction and shortening. Our model, however, do not allow us to distinguish between them, Twi regulatory pathways include the transcriptional activation of *fog,* and through the component A, the activation of RhoGEF2. Moreover, activation of *fog* and A results in actomyosin contractility through the same Rho GTPase activated pathway. Without adding a new component to the network that was exclusively under the control of Twi we should have assigned different activation states to the component A in order to differentiate apical from basolateral constriction. This approach is, however, inapplicable to the Boolean model proposed in this work, since each element of the network is considered to be either on or off, and intermediate expression levels are neglected. Cell shortening along the apicobasal axis may be dependent on the same machinery that generates apical cell constriction, which is the contraction of actomyosin network. To our knowledge, there is not information on specific mechanisms that regulate cell shortening, however it may be assumed that such mechanisms should be able to produce a functional activation of RhoGEF2 and Rho-GTPase along the lateral sides of the cells, while apical constriction is probably dependent on the apically localized activation of a GTPase.

A more direct role in the process of invagination has been suggested for Sna than for Twi. Experiments of over-expression of *sna*, in *twi* mutant background reveal that Sna induces at least part of the cell shape changes in the central cells of the VF, including apical constriction, given as result a discontinuous furrow that does not invaginate completely (Ip et al., 1994), due to the impairment in cell shortening as a consequence of *twi* absence (see below). It has been proposed by Ip et al. (1994) that *sna* promotes the activity of *twi* on mesoderm regulatory genes by blocking the expression of *twi* inhibitors that are normally restricted to the lateral neuroectoderm. A similar mechanism can be suggested to explain the effects of over-expressed *sna* on the cell shape changes, however there is no further biological evidence to support this regulatory mechanism. The analysis of *sna* and *twi* mutant cells indicates that nucleus movement from the apical to the basal cell side is under *sna* control, and we have represented it by a connection to B. As mentioned before (Section 3.3.1) we hypothesize that B might correspond to the small GTPase Rap1. The following evidence supports this assumption: in Rap1 mutant embryos there is a failure of the VF to close. In these embryos, VF cells display the apical constriction that is characteristic of the invaginating region. However, these cells are not brought together in the midline following VF formation and remain separated as two distinct rows. In these mutant embryos, nuclei are found at a variety of levels, and many of the nuclei fail to move basally as the VF forms (Asha et al., 1999).

Recent studies in mammalian tissue culture cells support the notion that Rap1 is a regulator of the cell morphology. Expression of a dominant-negative form of Rap1B is able to block the neuronal differentiation of PC12 cells in response to nerve growth factor (York et al., 1998). Rap1 is also activated to high levels during platelet aggregation, apparently in response to an increase in intracellular calcium (Franke et al., 1997). Additional evidence on the role of Rap1 in morphogenetic processes came from the report of Haigo et al. (2003). They demonstrated that Shroom an actin-binding protein expressed in epithelial cell is sufficient to bring about apical constriction during *Xenopus* neurulation. Interestingly, Shroom requires the activity of Rap1 to elicit this cell shape change. This protein is able to generate apical constriction in undifferentiated epithelial cells regardless of their presumptive fate, suggesting that in this case, as well in VF cells, the apical constriction requires the cellular machinery that is already in place in the epithelial cells. Even though, the mechanism that explains the activity of Rap1 in this morphogenetic process is unclear, these observations argue for a role for Rap1 in mediating certain morphological changes, possibly in response to several intracellular signaling pathways. It can be proposed that the interaction of Rap1 with a cytoskeletal component might require the binding of the activated Rap1 to an effector molecule, such as Shroom (Haigo et al., 2003) or AF-6, a linker protein, that translates Rap1 activation into cytoskeletal remodeling by recruiting the actin-regulator profilin to specific membrane domains of mammalian cells (Boettner et al., 2000).

In this work we attempted to understand the mechanisms that dictate the behavior of a single cell, since the concerted action of individual cells can drive

complex multicellular rearrangements. The description of VF formation at the level of cell sheets or coherent groups of cells, along with the incorporation of quantitative information to the model represents one of our future challenges. Nevertheless, the Boolean approach used in this work enabled us to integrate qualitative data on gene interactions into a coherent picture, and provided a straightforward method to verify the coherency of these interactions. Our analysis was focused on the structure and stable states of the regulatory network, which are not dependent on the type of updating of the network, however, in a future work, it might be possible to associate a certain type of updating to our model by using the accessible information of the activation schedule of some of the elements in the network. By doing so we might be able to study, for example, the dynamics trajectories of the different state configurations of the network.

Our work is in good agreement with known experimental results on wild type and mutant VF cells, revealing the internal robustness of the network and providing insights that might be relevant both from experimental and theoretical point of view. We concluded that new elements should be incorporated to the network and, at least for the element B, we proposed that it might correspond to the Rap1 GTPase. The analysis of a functional interaction between Sna and Rap1 GTPase, as well as, Rap1 over-expression experiments could help to verify this prediction. It is known that our understanding of the gene networks that control cellular behavior during gastrulation, and in particular, during VF formation is incomplete (Leptin, 1999; Ip and Gridley, 2002). This points to the limitations of classic genetic techniques, since mutants with a partially penetrate phenotype may be ignored and functionally redundant genes are entirely missed (Miklos and Rubin, 1996). As an alternative to the genetic approach, subtractive hybridization experiments that allowed the identification of genes differentially expressed during gastrulation (González-Agüero et al., 2005) and whole-genome microarray assays that identified a large number of new *Dorsal* target genes (Stathopoulos et al., 2002) have been reported, yielding insights into how the activity of transcripion factors and their associated signaling pathways control *Drosophila* VF formation during gastrulation.

Acknowledgments

This work was supported by Fondecyt 1010693 and 1050235 (VC), 1030618 (MG), and Fondap Matemáticas Aplicadas (JA). The authors would like to thank an anonymous referee for comments and suggestions that greatly improved the manuscript.

References

Albert, R., Othmer, H., 2003. The topology of the regulatory interactions predicts the expression pattern of the segment polarity genes in *Drosophila melanogaster*. J. Theor. Biol. 223, 1–18.

Amano, M., Ito, M., Kimura, K., Fukata, Y., Chihara, K., Nakano, T., Matsuura, Y., Kaibuchi, K., 1996. Phosphorylation and activation of myosin by Rho-associated kinase (Rho-kinase). J. Biol. Chem. 271, 20246–20249.

Aracena, J., Ben Lamine, S., Mermet, M.A., Cohen, O., Demongeot, J., 2002. Mathematical modelling in genetic networks. IEEE Trans. SMC Part B 33, 825–834.

Aracena, J., Demongeot, J., Goles, E., 2004. Positive and negative circuits in discrete neural networks. IEEE Trans. Neural Networks 15, 277–288.

Arbeitman, M.N., Furlong, E.E., Imam, F., Johnson, E., Null, B.H., Baker, B.S., Krasnow, M.A., Scott, M.P., Davis, R.W., White, K.P., 2002. Gene expression during the life cycle of *Drosophila melanogaster*. Science 297, 2270–2275.

Arthur, W.T., Petch, L.A., Burridge, K., 2000. Integrin engagement suppresses RhoA activity via a c-Src-dependent mechanism. Curr. Biol. 10, 719–722.

Asha, H., de Ruiter, N.D., Wang, M.G., Hariharan, I.K., 1999. The Rap1 GTPase functions as a regulator of morphogenesis in vivo. EMBO J. 18, 605–615.

Barrett, K., Leptin, M., Settleman, J., 1997. The Rho GTPase and putative RhoGEF mediate a signaling pathway for the cell shape changes in *Drosophila* gastrulation. Cell 91, 905–915.

Bodnar, J.W., 1997. Programming the *Drosophila* embryo. J. Theor. Biol. 188, 391–445.

Boettner, B., Govek, E.-E., Cross, J., Van aelst, L., 2000. The junctional multidomain protein AF-6 is a binding partner of the Rap1A GTPase and associates with the actin cytoskeletal regulator profilin. Proc. Natl Acad. Sci. USA 97, 9064–9069.

Boulay, J.L., Dennefeld, C., Alberga, A., 1987. The *Drosophila* developmental gene snail encodes a protein with nucleic acid binding fingers. Nature 330, 395–398.

Brouns, M.R., Matheson, S.F., Settleman, J., 2001. p190 RhoGAP is the principal Src substrate in brain and regulates axon outgrowth, guidance and fasciculation. Nat. Cell Biol. 3, 361–367.

Casares, F., Sanchez-Herrero, E., 1995. Regulation of the infra-abdominal regions of the bithorax complex of *Drosophila* by gap genes. Development 121, 1855–1866.

Chang, J.H., Gill, S., Settleman, J., Parsons, S.J., 1995. c-Src regulates the simultaneous rearrangement of actin cytoskeleton, p190RhoGAP, and p120RasGAP following epidermal growth factor stimulation. J. Cell Biol. 130, 355–368.

Costa, M., Sweeton, D., Wieschaus, E., 1993. Gastrulation in *Drosophila*: cellular mechanisms of morphogenetic movements. In: Bate, M., Martinez-Arias, A. (Eds.), The Development of *Drosophila*. Cold Spring Harbor Laboratory Press, Cold Spring Harbor, New York, pp. 425–466.

Costa, M., Wilson, E., Wieschaus, E., 1994. A putative cell signal encoded by the folded gastrulation gene coordinates cell shape changes during *Drosophila* gastrulation. Cell 76, 1075–1089.

Crawford, J.M., Harden, N., Leung, T., Lim, L., Kiehart, D.P., 1998. Cellularization in *Drosophila* melanogaster is disrupted by the inhibition of rho activity and the activation of Cdc42 function. Dev. Biol. 204, 151–164.

Demongeot, J., Aracena, J., Thuderoz, F., Baum, T.P., Cohen, O., 2003. Genetic regulation networks: circuits, regulons and attractors. C. R. Biol. 326, 171–188.

Franke, B., Akkerman, J.W., Bos, J.L., 1997. Rapid Ca^{2+}-mediated activation of Rap1 in human platelets. EMBO J. 16, 252–259.

Fukata, Y., Kimura, K., Oshiro, N., Saya, H., Matsuura, Y., Kaibuchi, K., 1998. Association of the myosin-binding subunit of

myosin phosphatase and moesin: dual regulation of moesin phosphorylation by Rho-associated kinase and myosin phosphatase. J. Cell Biol. 141, 409–418.

Gaul, U., Mardon, G., Rubin, G.M., 1992. A putative Ras GTPase activating protein acts as a negative regulator of signaling by the Sevenless receptor tyrosine kinase. Cell 68, 1007–1019.

Goles, E., Martínez, S., 1991. Neural and Automata Networks, Mathematics and its Applications Series, vol. 58. Kluwer Academic Publishers, Dordrecht 264pp.

Gong, L., Puri, M., Unlu, M., Young, M., Robertson, K., Viswanathan, S., Krishnaswamy, A., Dowd, S.R., Minden, J.S., 2004. *Drosophila* ventral furrow morphogenesis: a proteomic analysis. Development 131, 643–656.

González-Agüero, M., Zúñiga, A., Pottstock, H., Del Pozo, T., González, M., Cambiazo, V., 2005. Identification of genes expressed during *Drosophila melanogaster* gastrulation by using subtractive hybridization. Gene 345, 213–224.

Häcker, U., Perrimon, N., 1998. DRhoGEF2 encodes a member of the dbl family of oncogenes and controls cell shape changes during gastrulation in *Drosophila*. Genes Dev. 12, 274–284.

Haigo, S.L., Hildebrand, J.D., Harland, R.M., Wallingford, J.B., 2003. Shroom induces apical constriction and is required for hingepoint formation during neural tube closure. Curr. Biol. 13, 2125–2137.

Halsell, S.R., Chu, B.I., Kiehart, D.P., 2000. Genetic analysis demonstrates a direct link between rho signaling and nonmuscle myosin function during *Drosophila* morphogenesis. Genetics 155, 1253–1265.

Harden, N., Loh, H.Y., Chia, W., Lim, L., 1995. A dominant inhibitory version of the small GTP-binding protein Rac disrupts cytoskeletal structures and inhibits developmental cell shape changes in *Drosophila*. Development 121, 903–914.

Hart, M., Jiang, X., Kozasa, T., Roscoe, W., Singer, W., Gilman, A., Sternweis, P., Bollag, G., 1998. Direct stimulation of the guanine nucleotide exchange activity of p115 RhoGEF by G 13. Science 280, 2112–2114.

Hemavathy, K., Meng, X., Ip, Y.T., 1997. Differential regulation of gastrulation and neuroectodermal gene expression by Snail in the *Drosophila* embryo. Development 124, 3683–3691.

Hirao, M., Sato, N., Kondo, T., Yonemura, S., Monden, M., Sasaki, T., Takai, Y., Tsukita, Sh., Tsukita, Sa., 1996. Regulation mechanism of ERM (ezrin/radixin/moesin) protein/plasma membrane association: possible involvement of phosphatidylinositol turnover and Rho-dependent signaling pathway. J. Cell Biol. 135, 37–51.

Huang, S., 1999. Gene expression profiling, genetic networks and cellular states: an integrating concept for tumorigenesis and drug discovery. J. Mol. Med. 77, 469–480.

Ip, Y.T., Gridley, T., 2002. Cell movements during gastrulation: snail dependent and independent pathways. Curr. Opin. Genet. Dev. 12, 423–429.

Ip, Y.T., Maggert, K., Levine, M., 1994. Uncoupling gastrulation and mesoderm differentiation in the *Drosophila* embryo. EMBO J. 13, 5826–5834.

Jiang, J., Kosman, D., Ip, Y.T., Levine, M., 1991. The dorsal morphogen gradient regulates the mesoderm determinant twist in early Drosophila embryos. Genes Dev. 5, 1881–1891.

Kam, Z., Minden, J.S., Agard, D.A., Sedat, J.W., Leptin, M., 1991. *Drosophila* gastrulation: analysis of cell shape changes in living embryos by three-dimensional fluorescence microscopy. Development 112, 365–370.

Kauffman, S., 1969. Metabolic stability and epigenesis in randomly constructed genetics nets. J. Theor. Biol. 22, 437–467.

Kauffman, S.A., 1993. The Origins of Order, Self-Organization and Selection in Evolution. Oxford University Press, Oxford.

Kiehart, D.P., 1990. The actin membrane skeleton in *Drosophila* development. Semin. Cell Biol. 1, 325–339.

Kikuchi, A., Kuroda, S., Sasaki, T., Kotani, K., Hirata, K., Katayama, M., Takai, Y., 1992. Functional interactions of stimulatory and inhibitory GDP/GTP exchange proteins and their common substrate small GTP-binding protein. J. Biol. Chem. 267, 14611–14615.

Kimura, K., Ito, M., Amano, M., Chihara, K., Fukata, Y., Nakafuku, M., Yamamori, B., Feng, J., Nakano, T., Okawa, K., Iwamatsu, A., Kaibuchi, K., 1996. Regulation of myosin phosphatase by Rho and Rho-associated kinase (Rho-kinase). Science 273, 245–248.

Kosman, D., Ip, Y.T., Levine, M., Arora, K., 1991. Establishment of the mesoderm-neuroectoderm boundary in the *Drosophila* embryo. Science 254, 118–122.

Kozasa, T., Jiang, X., Hart, M., Sternweis, P., Singer, W., Gilman, A., Bollag, G., Sternweis, P., 1998. p115 RhoGEF, a GTPase activating protein for G alpha 12 and G alpha 13. Science 280, 2109–2111.

Kureishi, Y., Kobayashi, S., Amano, M., Kimura, K., Kanaide, H., Nakano, T., Kaibuchi, K., Ito, M., 1997. Rho-associated kinase directly induces smooth muscle contraction through myosin light chain phosphorylation. J. Biol. Chem. 272, 12257–12260.

Kuroda, S., Kikuchi, A., Hirata, K., Masuda, T., Kishi, K., Sasaki, T., Takai, Y., 1992. Cooperative function of rho GDS and rho GDI to regulate rho p21 activation in smooth muscle. Biochem. Biophys. Res. Commun. 185, 473–480.

Leptin, M., 1991. twist and snail as positive and negative regulators during *Drosophila* mesoderm development. Genes Dev. 5, 1568–1576.

Leptin, M., 1995. Drosophila gastrulation: from pattern formation to morphogenesis. Annu Rev. Cell Dev. Biol. 11, 189–212.

Leptin, M., 1999. Gastrulation in *Drosophila*: the logic and the cellular mechanisms. EMBO J. 18, 3187–3192.

Leptin, M., Grunewald, B., 1990. Cell shape changes during gastrulation in *Drosophila*. Development 110, 73–84.

Leptin, M., Roth, S., 1994. Autonomy and non-autonomy in *Drosophila* mesoderm determination and morphogenesis. Development 120, 853–859.

Lowry, W.E., Huang, J., Ma, Y.C., Ali, S., Wang, D., Williams, D.M., Okada, M., Cole, P.A., Huang, X.Y., 2002. Csk, a critical link of g protein signals to actin cytoskeletal reorganization. Dev. Cell 2, 733–744.

Margolis, J.S., Borowsky, M.L., Steingrimsson, E., Shim, C.W., Lengyel, J.A., Posakony, J.W., 1995. Posterior stripe expression of hunchback is driven from two promoters by a common enhancer element. Development 121, 3067–3077.

Matsui, T., Maeda, M., Doi, Y., Yonemura, S., Amano, M., Kaibuchi, K., Tsukita, S., Tsukita, S., 1998. Rho-kinase phosphorylates COOH-terminal threonines of ezrin/radixin/moesin (ERM) proteins and regulates their head-to-tail association. J. Cell Biol. 140, 647–657.

Mendoza, L., Alvarez-Buylla, E., 1998. Dynamics of the genetic regulatory network for *Arabidopsis thaliana* flower morphogenesis. J. Theor. Biol. 193, 307–319.

Miklos, G.L., Rubin, G.M., 1996. The role of the genome project in determining gene function: insights from model organisms. Cell 86, 521–529.

Miller, M.A., Malik, I.A., Shenk, M.A., Steele, R.E., 2000. The Src/Csk regulatory circuit arose early in metazoan evolution. Oncogene 19, 3925–3930.

Mizuno, T., Tsutsui, K., Nishida, Y., 2002. *Drosophila* myosin phosphatase and its role in dorsal closure. Development 129, 1215–1223.

Morize, P., Christiansen, A.E., Costa, M., Parks, S., Wieschaus, E., 1998. Hyperactivation of the folded gastrulation pathway induces specific cell shape changes. Development 125, 589–597.

Morrison, D.K., Murakami, M.S., Cleghon, V., 2000. Protein kinases and phosphatases in the *Drosophila* genome. J. Cell Biol. 150, F57–F62.

Okada, M., Nada, S., Yamanashi, Y., Yamamoto, T., Nakagawa, H., 1991. CSK: a protein-tyrosine kinase involved in regulation of src family kinases. J. Biol. Chem. 266, 24249–24252.

Parks, S., Wieschaus, E., 1991. The *Drosophila* gastrulation gene concertina encodes a Ga-like protein. Cell 64, 447–458.

Piekny, A.J., Mains, P.E., 2002. Rho-binding kinase (LET-502) and myosin phosphatase (MEL-11) regulate cytokinesis in the early *Caenorhabditis elegans* embryo. J. Cell Sci. 115, 2271–2282.

Piekny, A.J., Wissmann, A., Mains, P.E., 2000. Embryonic morphogenesis in *Caenorhabditis elegans* integrates the activity of LET-502 Rho-binding kinase, MEL-11 myosin phosphatase, DAF-2 insulin receptor and FEM-2 PP2c phosphatase. Genetics 156, 1671–1689.

Priess, J.R., Hirsh, D.I., 1986. *Caenorhabditis elegans* morphogenesis: the role of the cytoskeleton in elongation of the embryo. Dev. Biol. 117, 156–173.

Sánchez, L., Thieffry, D., 2001. A logical analysis of the Drosophila Gap-gene System. J. Theor. Biol. 211, 115–141.

Sánchez, L., Thieffry, D., 2003. Segmenting the fly embryo: a logical analysis of the pair-rule cross-regulatory module. J. Theor. Biol. 224, 517–537.

Sánchez, L., van Helden, J., Thieffry, D., 1997. Establishement of the dorso-ventral pattern during embryonic development of drosophila melanogasater: a logical analysis. J. Theor. Biol. 189, 377–389.

Sasaki, T., Takai, Y., 1998. The Rho small G protein family-Rho GDI system as a temporal and spatial determinant for cytoskeletal control. Biochem. Biophys. Res. Commun. 28 pp. 245, 641–645.

Sauer, F., Rivera-Pomar, R., Hoch, M., Jackle, H., 1996. Gene regulation in the *Drosophila* embryo. Philos. Trans. R. Soc. Lond. B Biol. Sci. 351, 579–587.

Simons, P.C., Pietromonaco, S.F., Reczek, D., Bretscher, A., Elias, L., 1998. C-terminal threonine phosphorylation activates ERM proteins to link the cell's cortical lipid bilayer to the cytoskeleton. Biochem. Biophys. Res. Commun. 253, 561–565.

Snoussi, E.H., Thomas, R., 1993. Logical identification of all steady states: the concept of feedback loop characteristic states. Bull. Math. Biol. 55, 973–991.

Somlyo, A.P., Somlyo, A.V., 2003. Ca2+ sensitivity of smooth muscle and nonmuscle myosin II: modulated by G proteins, kinases, and myosin phosphatase. Physiol. Rev. 83, 1325–1358.

Somogyi, R., Sniegoski, C.A., 1996. Modeling the complexity of genetic networks: understanding multigenic and pleiotropic regulation. Complexity 1, 45–63.

Stathopoulos, A., Van Drenth, M., Erives, A., Markstein, M., Levine, M., 2002. Whole-genome analysis of dorsal–ventral patterning in the *Drosophila* embryo. Cell 111, 687–701.

Sweeton, D., Parks, S., Costa, M., Wieschaus, E., 1991. Gastrulation in *Drosophila*: the formation of the ventral furrow and posterior midgut invaginations. Development 112, 775–789.

Takahashi, K., Sasaki, T., Mammoto, A., Takaishi, K., Kameyama, T., Tsukita, S., Takai, Y., 1997. Direct Interaction of the Rho GDP Dissociation Inhibitor with Ezrin/Radixin/Moesin Initiates the Activation of the Rho Small G Protein. J. Biol. Chem. 272, 23371–23375.

Tan, C., Stronach, B., Perrimon, N., 2003. Roles of myosin phosphatase during *Drosophila* development. Development 130, 671–681.

Thieffry, D., Sánchez, L., 2003. Dynamical modelling of pattern formation during embryonic development. Curr. Opin. Gen. Dev. 13, 326–330.

Thieffry, D., Snoussi, E.H., Richelle, J., Thomas, R., 1995. Positive loops and differentiation. J. Biol. Syst. 3, 457–466.

Thomas, R., Thieffry, D., Kaufman, M., 1995. Dynamical behaviour of biological regulatory networks-I. Biological role of feedback loops and practical use of the concept of loop-characteristic state. Bull. Math. Biol. 57, 247–276.

Tsukita, S., Yonemura, S., 1999. Cortical actin organization: lessons from ERM (ezrin/radixin/moesin) proteins. J. Biol. Chem. 274, 34507–34510.

Van Aelst, L., Symons, M., 2002. Role of Rho family GTPases in epithelial morphogenesis. Genes Dev. 16, 1032–1054.

Winter, C.G., Wang, B., Ballew, A., Royou, A., Karess, R., Axelrod, J.D., Luo, L., 2001. *Drosophila* Rho-associated kinase (Drok) links Frizzled-mediated planar cell polarity signaling to the actin cytoskeleton. Cell 105, 81–91.

Wissmann, A., Ingles, J., McGhee, J.D., Mains, P.E., 1997. *Caenorhabditis elegans* LET-502 is related to Rho-binding kinases and human myotonic dystrophy kinase and interacts genetically with a homolog of the regulatory subunit of smooth muscle myosin phosphatase to affect cell shape. Genes Dev. 11, 409–422.

Wissmann, A., Ingles, J., Mains, P.E., 1999. The Caenorhabditis elegans mel-11 myosin phosphatase regulatory subunit affects tissue contraction in the somatic gonad and the embryonic epidermis and genetically interacts with the Rac signaling pathway. Dev Biol. 209, 111–127.

Wuensche, A., 1998. Genomic regulation modeled as a network with basins of attraction. Pac. Symp. Biocomput., 89–102.

Yau, D.M., Yokoyama, N., Goshima, Y., Siddiqui, Z.K., Siddiqui, S.S., Kozasa, T., 2003. Identification and molecular characterization of the G alpha12-Rho guanine nucleotide exchange factor pathway in *Caenorhabditis elegans*. Proc. Natl Acad. Sci. USA 100, 14748–14753.

York, R.D., Yao, H., Dillon, T., Ellig, C.L., Eckert, S.P., Mccleskey, E.W., Stork, P.J., 1998. Rap1 mediates sustained MAP kinase activation induced by nerve growth factor. Nature 392, 622–626.

Young, P.E., Pesacreta, T.C., Kiehart, D.P., 1991. Dynamic changes in the distribution of cytoplasmic myosin during *Drosophila* embryogenesis. Development 111, 1–14.

Zuckerkandl, E., 1994. Molecular pathways to parallel evolution: I. Gene nexuses and their morphological correlates. J. Mol. Evol. 39, 661–678.